Microporous and Mesoporous Materials 305 (2020) 110192

Contents lists available at ScienceDirect

Microporous and Mesoporous Materials

journal homepage: http://www.elsevier.com/locate/micromeso

Green synthesis of MCM-41 from rice husk and its functionalization with nickel(II) salen complex for the rapid catalytic oxidation of benzyl alcohol

Salih Hamza Abbas [a,b], Farook Adam [a], Lingeswarran Muniandy [a,*]

[a] School of Chemical Sciences, Universiti Sains Malaysia, 11800, Penang, Malaysia
[b] Department of Chemistry, College of Science, University of Basrah, 61004, Basrah, Iraq

ARTICLE INFO

Keywords:
Rice husk
Mesoporous silica
Nickel
Oxidation
Benzyl alcohol

ABSTRACT

N,N′-bis(4-hydroxysalicylidene)ethylenediamine nickel(II) complex was synthesized and functionalized onto MCM-41. The catalyst denoted as MCMSalenNi, was found to retain its hexagonal mesoporous structure as indicated from the TEM images. It however, had a reduced surface area and lower x-ray diffraction intensity than the parent MCM-41. Both FT-IR and solid-state MAS NMR (^{29}Si, ^{13}C) analyses proved that the complex was successfully functionalized onto the MCM-41 support. The catalyst was used in the rapid oxidation of benzyl alcohol and it afforded a high conversion (~98%) with benzaldehyde as the major product within 90 min. Periodic acid was used as a mild oxidant. In addition, the catalyst was reused up to six times with minimal loss of activity.

1. Introduction

Organic synthesis plays a major role in producing new compounds that can be used to make products which are important in our daily lives [1–3]. Therefore, it is important for us to come up with an environmental friendly and cost-effective method for the synthesis of important organic compounds. One such compound which has wide applications is benzaldehyde. Benzaldehyde is the simplest aromatic aldehyde and it is extensively used in the food and cosmetic industry [4]. Apart from that, it is also used to manufacture aniline and acridine dyes [5]. Benzaldehyde is produced mainly via the liquid phase chlorination and oxidation of toluene; whereas, the natural synthesis method involves the aldol reaction of cinnamaldehyde, usually obtained from cassia oil [6,7]. This method however, produces acetaldehyde as a by-product requiring extensive reaction time (5–80 h) and high temperatures (90–150 °C) [6]. Consequently, an efficient approach is required for the sustainable production of benzaldehyde. One such method is via the catalytic oxidation of benzyl alcohol.

Rice husk (RH) is a waste material found in abundance especially in Asian countries due to the daily dietary intake of rice. Rice husk ash (RHA) possesses high silica content making it a suitable precursor for the synthesis of mesoporous silica; thereby giving added value to waste byproducts from the rice milling industry [8]. In the past, rice husk RH was used as landfills or burnt openly as a way of disposal. Open burning of RH is detrimental to the environment and also caused silicosis in the people living nearby [9]. Earlier reports show that RH can be used to prepare silica and is a viable starting material for the synthesis of support materials which are widely used in heterogeneous catalysis such as MCM-41, SBA-16 and also zeolite [10–12].

Several key methods of incorporating active materials onto inert support samples had been reported previously. Wet impregnation, co-precipitation and surface functionalization are some of the well-known techniques used in the development of heterogeneous catalysis [13–15]. There are some reports on the use of transition metals in the catalytic oxidation of benzyl alcohol. Thao and Nu [16] had utilized several metal oxides deposited on sepiolite and used it for the synthesis of benzaldehyde. They obtained a maximum conversion of 60–70% with 99% selectivity for benzaldehyde. However, the catalyst requires 10 h of reaction time. Sultana et al. [17] used a trimetallic catalyst (ytterbia doped mixed Ni–Mn oxides) for the same reaction and successfully obtained 100% conversion of benzyl alcohol with >99% selectivity towards benzaldehyde, despite requiring a reaction time of 5 h. Kimi et al. [18] studied the effectiveness of Cu–Ni nanoparticles supported on activated carbon prepared by wet impregnation technique and managed to obtain 46.8% conversion of benzyl alcohol within 2 h. Some of the previous work carried out on the oxidation of benzyl alcohol is listed in Table 1.

The presence of silanol groups (Si–OH) on silica is important to

* Corresponding author.
E-mail address: warran873@gmail.com (L. Muniandy).

https://doi.org/10.1016/j.micromeso.2020.110192
Received 12 January 2020; Received in revised form 7 March 2020; Accepted 31 March 2020
Available online 8 April 2020

Table 1
Summary of previous work on the oxidation of benzyl alcohol in comparison to the present study.

Catalyst/s	Conversion of benzyl alcohol (%)	Reaction conditions and duration
Cr/Sepiolite [16]	~60-70	50–70 °C, *t*-butyl hydrogen peroxide as oxidant, 600 min
Yb_2O_3(5%)-Ni_6MnO_8 [17]	100	100 °C, oxygen gas as oxidant, 300 min
$CuNi_1$/AC [18]	46.8	80 °C, hydrogen peroxide as oxidant, 120 min
Pt/ZnO [19]	94.1	26 °C, aqueous conditions under open air, 600 min
Mn-3-300 (MnO supported on MCM-41) [20]	94.0	80 °C, hydrogen peroxide as oxidant,720 min
2.0Sm/0.5Au/$Ce_{0.5}Zr_{0.5}O_2$ [21]	95.0	90 °C, oxygen gas as oxidant,720 min
MCMSalenNi [Present study]	98.4	90 °C, periodic acid as oxidant, 90 min

anchor the functional groups onto its surface [22]. In this particular study however, nickel(II) salen complex was functionalized using 3-chloropropyltriethoxysilane (CPTES) as an alkylating agent onto MCM-41. The MCM-41 was synthesized from RH. This catalyst was denoted as MCMSalenNi, and used to study the rapid oxidation of benzyl alcohol with periodic acid (H_5IO_6) as a mild oxidant.

2. Experimental

2.1. Materials

The RH was obtained from a rice mill in Penang. Other chemicals used were cetyltrimethylammonium bromide (Merck, 95%), nickel acetate/Ni(OAc)$_2$·4H$_2$O (Merck, 98%), 3-chloropropyltriethoxysilane (Aldrich, 99.8%), triethylamine (Aldrich, 99%), 4-hydroxysalicylaldehyde (Aldrich, 98%), 1,2-diaminoethane (Aldrich, 99.5), toluene (Qrec, 99.5%), methanol (Qrec, 99.8%), ethanol (Qrec, 99.7%), acetonitrile (Qrec, 99.5%), dichloromethane (Qrec, 99.5%), nitric acid (Qrec, 69%), benzyl alcohol (Unilab, 97%) and periodic acid (R&M Chemicals, 99.5%). All chemicals were of analytical grade and used without purification.

2.2. Preparation of catalyst

2.2.1. Preparation of RHA and MCM-41

Pure amorphous silica was obtained from RH using the method reported previously [23,24]. The RH was first washed with copious amount of water to remove solid particles, mud and soil. It was allowed to dry before being treated with 1.0 M nitric acid for 24 h. The acid treated RH was then rinsed with distilled water until neutrality before drying at room temperature for 24 h. It was later calcined at 800 °C in a muffle furnace for 6 h yielding fine white powder which was labelled as RHA. MCM-41 was prepared following the method reported elsewhere [25,26], by weighing 4.0 g of RHA into a round bottom flask containing 200 mL of 2.0 M NaOH solution at 70 °C and maintained for 24 h. The resulting sodium silicate was later filtered and added dropwise into a Nalgene bottle which contained CTAB solution (4.6 g of CTAB dissolved in 25 g of H$_2$O) at room temperature. The pH of the sample was adjusted to ~10 using 1.0 M acetic acid and incubated at 100 °C in the oven for 96 h and continuously monitored every 24 h. Following that, the mixture was taken out from the oven and allowed to cool and aged at room temperature for 24 h. The sample was filtered, rinsed with distilled water-ethanol mixture before being oven dried at 105 °C for 24. It was later calcined at 450 °C for 5 h to remove the CTAB.

2.2.2. The functionalization of MCM-41

The functionalization of MCM-41 was done according to the method reported by Sutra and Brunel [25]. Initially, MCM-41 (~1.0 g) was oven dried at 110 °C for 3 h to assist in the removal of physisorbed moisture before being added to CPTES (1.0 mL) in dry toluene (30 mL). The mixture was refluxed with stirring under dry argon for 24 h. The mixture was then filtered, yielding a white solid denoted as Cl-MCM-41 (yield = 1.13 g), which was rinsed with dry toluene followed by ethanol and dried at 70 °C overnight.

2.2.3. Synthesis of Schiff base (N,N′-bis(4-hydroxysalicylidene) ethylenediamine)

4-hydroxysalicylaldehyde (4.0 g, 29 mmol) was dissolved in 6 mL of ethanol and added dropwise into 1,2-diaminoethane (0.87 g, 14.5 mmol) which was dissolved in 7.0 mL of ethanol. The mixture was later refluxed for 4 h. A yellow-orange precipitate was observed which was due to the formation of the symmetric Schiff-base ligand H$_2$((OH)$_2$-salen). The product was separated via suction filtration, rinsed and recrystallized using ethanol. It was later dried in vacuum. Yield: 4.12 g, 94.74%; appearance: yellow-orange solid; m.p.: >230 °C; FT-IR (KBr pellet, cm^{-1}): the band at 1640 cm^{-1} was assigned to the C═N bond whereas another band at 1582 cm^{-1} was assigned to the C–O bond; ^{1}H NMR (300 MHz, DMSO-d_6, ppm) δ 3.76 (s, CH$_2$–N, 4H); 6.14 (s, Ar-CH, 2H); 6.24 (d, J = 2.67 Hz, Ar-CH, 2H); 7.15 (d, J = 6.56 Hz, Ar-CH, 2H); 8.35 (s, CH═N, 2H) and 13.6 (s, OH, 4H).

2.2.4. Synthesis of N,N′-bis(4-hydroxysalicylidene)ethylenediamine nickel (II) complex

N,N'-bis(4-hydroxysalicyclidene)ethylenediamine nickel(II) complex was prepared according to the method reported elsewhere [26]. Initially, Ni(OAc)$_2$.4H$_2$O (1.24 g, 4.0 mmol) was dissolved in 10.0 mL of distilled water. This solution was later added to the refluxing solution of N,N'-bis(2,4-dihydroxybenzaldehyde)ethylenediamine (1.5 g, 4.0 mmol in 10.0 mL of ethanol at ~ 90 °C). A red precipitate appeared immediately, and the mixture was allowed to reflux for 2 h. The reddish precipitate was filtered out and washed with equal amount of water/ethanol mixture followed by diethyl ether to yield N,N′-bis (4-hydroxysalicylidene)ethylenediamine nickel(II) complex. This complex was denoted as Ni(4-OH)$_2$ salen. Yield: 1.7 g, 95.6%; appearance: red solid; m.p.: >230 °C; FT-IR (KBr pellet, cm^{-1}): The C═N vibration band at 1640 cm^{-1} red shifted to 1617 cm^{-1}, while the C–O vibration band at 1000 cm^{-1} was blue shifted to 1300 cm^{-1} after complexation of H$_2$((OH)$_2$-salen) with nickel(II) cation as observed in Fig. 1. This implies

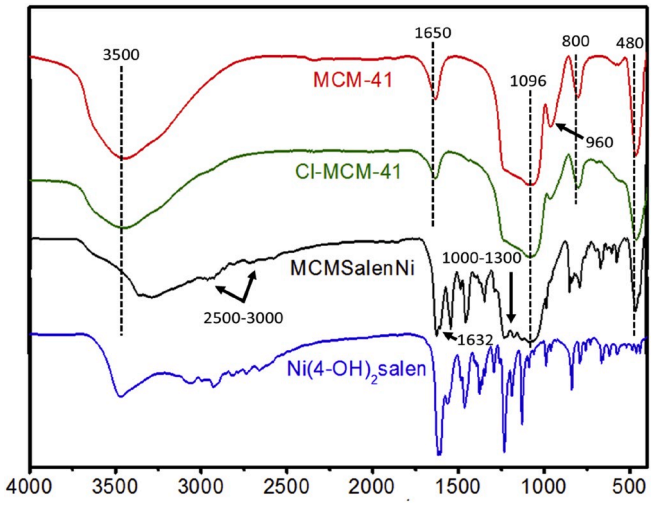

Fig. 1. The FT-IR spectra of the samples prepared in the present study.

that the nickel cation was coordinated to the ligand via the two N and O donor atoms as a tetradentate ONNO complex [27–29]; ^{1}H NMR (300 MHz, DMSO-d_6, ppm) δ 3.39 (s, CH_2–N, 4H); 6.028 (d, J = 3.03 Hz, Ar-CH, 2H); 6.055 (s, Ar-CH, 2H); 7.05 (d, J = 7.59 Hz, Ar-CH, 2H); 7.62 (s, CH═N, 2H) and 9.74 (s, OH, 2H); these results agreed with the reported experimental details [26]; ^{13}C NMR (500 MHz, DMSO-d_6, ppm): δ 58.5, 104.5, 106.4, 114.9, 134.9, 161.8, 163.3 and 166.5.

2.2.5. Functionalization of N,N′-bis(4-hydroxysalicylidene) ethylenediimine-nickel (II) complex onto Cl-MCM-41

Approximately 1.0 g of Cl-MCM-41 was weighed into a round bottom flask containing triethylamine (0.568 g, 5.6 mmol) in dry toluene (30 mL). Then, 1.0 g (2.8 mmol) of the nickel(II) complex was added and the mixture was refluxed for 48 h at 110 °C. The resultant suspension was then filtered and washed with dry toluene before being oven dried at 110 °C overnight. The dried sample was placed in a desiccator for further analysis and denoted as MCMSalenNi. Yield: 1.2 g. Scheme 1

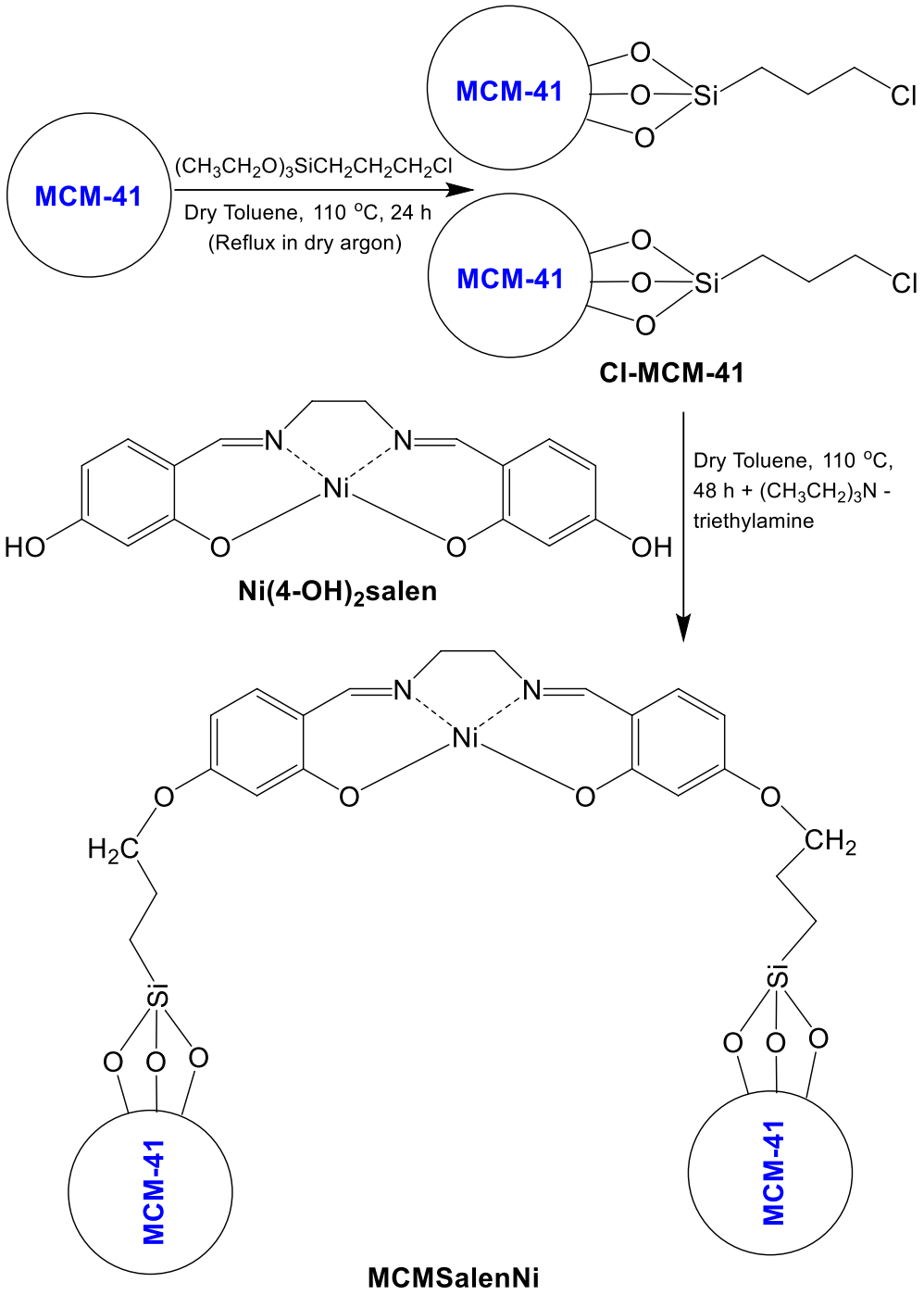

Scheme 1. The synthesis of MCMSalenNi using CPTES as anchoring agent.

Table 2
The conditions programmed for the analysis of the reactants and products using GC-FID and GC-MS.

Parameter	GC-FID	GC-MS
Initial temperature (°C)	50	50
Initial time (min)	0	0
Ramp 1 (°C min^{-1})	15	15
Temperature 1 (°C)	150	150
Hold 1 (min)	0	0
Final temperature (°C)	230	230
Final ramp (°C min^{-1})	20	20
Final hold (min)	2	2
Total time (min)	12.6	12.6
Injection temperature (°C)	200	200
Detection temperature (°C)	240	240
Carrier gas	Nitrogen	Helium
Flow rate (mL min^{-1})	2	2

depicts the whole process for the synthesis of this catalyst.

2.3. Catalyst characterization

The catalyst was characterized using FT-IR (PerkinElmer System 2000), powder x-ray diffraction (Siemens Diffractometer D5000, Kristalloflex using CuKα radiation, λ = 0.154 nm, voltage = 40 kV, current = 30 mA), N_2 adsoption-desoprtion porosimetry (Micromeritics ASAP 2020 Porosimeter with a degassing condition of 200 °C for 12h), atomic absorption spectroscopy (PerkinElmer A Analyst 200), ^{13}C and ^{29}Si solid state MAS NMR spectrometer (Bruker AVANCE III, 400 MHz). The TEM and SEM images were obtained from transmission electron microscopy (TEM, Phillips CM12) and scanning electron microscopy (SEM, Leo Supra 50 VP) fitted with energy dispersive x-ray spectrometer (EDAX Falcon system).

2.4. Catalytic oxidation of benzyl alcohol

In a typical catalytic run, ~0.05 g of the catalyst (MCMSalenNi) was weighed into a 25 mL two necked round bottom flask which contained benzyl alcohol (0.108 g, 1.0 mmol), periodic acid (oxidant, 0.227 g, 1.0 mmol), cyclohexanone (internal standard, 10 μL) and acetonitrile (solvent, 12.0 mL). The reactants were magnetically stirred and refluxed for the required duration. The yield and conversion of the reaction was determined using gas chromatography (GC-FID, PerkinElmer Clarus 500) equipped with Elite Wax column. Identification of the products, however, was done using gas chromatography-mass spectrometer (GC-MS, PerkinElmer Clarus 600) fitted with Elite 5 column. The parameters for the analysis using GC-FID/MS are summarized in Table 2. The percentage conversion of benzyl alcohol was calculated from equation (1);

$$\%\ conversion = (1 - [\frac{C_t}{C_0}])\ x\ 100\% \quad (1)$$

Where, C_0 refers to the initial concentration of benzyl alcohol while C_t is the concentration of benzyl alcohol at selected time intervals.

2.5. Leaching and reusability studies

The leaching test was performed to determine the heterogeneity of MCMSalenNi. The catalyst was filtered off after 15 min of the reaction (optimized condition). The remainder of the reaction was then allowed to proceed without the presence of the catalyst. For the reusability studies however, the catalyst was collected after each run, washed thoroughly with water, chloroform and diethyl ether before being vacuum dried at 70 °C for 24 h. Then, it would be subjected for the oxidation of benzyl alcohol under the optimized condition. This cycle was repeated several times.

3. Result and discussion

3.1. Characterization of the prepared samples

3.1.1. FT-IR analysis

The FT-IR analysis of the samples prepared in the present study is shown in Fig. 1. The spectra indicate the changes taking place in MCM-41 upon functionalization with Ni(4-OH)$_2$ salen complex. The FT-IR spectrum for MCM-41 exhibited several bands typical for mesoporous silica. A broad band was observed in the vicinity of ~3500 cm^{-1} due to the presence of hydroxyl (–O–H) vibration of the silanol groups (Si–OH) [30]. The band at ~1630 cm^{-1} was due to the bending vibration of trapped water molecules [30].

The broad band observed at ~1096 cm^{-1} was due to the asymmetric vibration of the siloxane (Si–O–Si) bonds [31]. In addition, a sharp band was observed at ~960 cm^{-1} which is due to the symmetric stretching of the silanol (Si–OH) bonds [31]. The bands at ~800 and 480 cm^{-1} were due to the stretching and bending modes of siloxane groups [32]. For Cl-MCM-41, the intensity of the band corresponding to the silanol groups (Si–OH) at ~ 960 cm^{-1} reduced significantly indicating successful anchoring of CPTES [31]. However, bands at ~2800-2900 cm^{-1} which should be due to the C–H bonds from CPTES were not clearly visible and appeared as small humps instead. The FT-IR spectrum for MCMSalenNi however, showed some changes after the functionalization with Ni(4-OH)$_2$ salen complex. Firstly, the broad band corresponding to the O–H vibration was shifted to ~3400 cm^{-1}. Additionally, clusters of low intensity bands were noted in the region between ~3000 and 2500 cm^{-1} due to the aliphatic and aromatic C–H stretching vibrations of the ligand [30]. The band at ~1632 cm^{-1} is attributed to the C═N vibration of the Ni(4-OH)$_2$ salen complex indicating successful functionalization of the ligand onto MCM-41 [33]. The bands due to C–O vibrations usually appear in the vicinity of 1000–1300 cm^{-1} as can be seen in the FT-IR spectrum of Ni(4-OH)$_2$ salen complex [34]. However, after functionalization with MCM-41, these bands overlapped with that of the siloxane group (Si–O–Si), although relatively small bands still appeared as exhibited from the FT-IR spectrum of MCMSalenNi.

3.1.2. ^{13}C and ^{29}Si MAS NMR analysis of MCMSalenNi

The immobilized nickel(4-OH)$_2$ salen complex has 11 symmetrically connected carbon atoms as shown in the ^{13}C MAS NMR spectra of MCMSalenNi (Fig. 2a). These chemical shifts were observed at 7.4, 26.1, 45.5, 54.9, 104.6, 107.5, 116.7, 136.7, 161.4, 163.7 ppm and assigned as indicated in Fig. 2a. However, the chemical shift for C7 was not observed in the spectrum due to overlap with the chemical shift for C6. Despite this, the chemical shift for C7 was observed in the liquid state ^{13}C NMR of Ni(4-OH)$_2$ salen complex as shown in Fig. 3. This is not surprising as it is very restrictive in the solid state, where overlapping of the chemical shift is highly possible.

The ^{29}Si MAS NMR spectra of MCMSalenNi exhibited several chemical shifts as shown in Fig. 2b. Three peaks were observed correlating to the T^2 (−57.8 ppm), T^3 (−67.1 ppm) and Q^4 (−110.3 ppm) chemical shifts respectively. The presence of organosilane moieties are proven from the presence of T^2 and T^3 peaks [$T^m = RSi(OSi)_m(OH)_{3-m}$, m = 1–3]. Whereas, the Q^4 peak [$Q^n = Si(OSi)_n(OH)_{4-n}$, n = 2–4] denotes the presence of siloxane ($Si(OSi)_4$) units [35]. However, Q^2 and Q^3

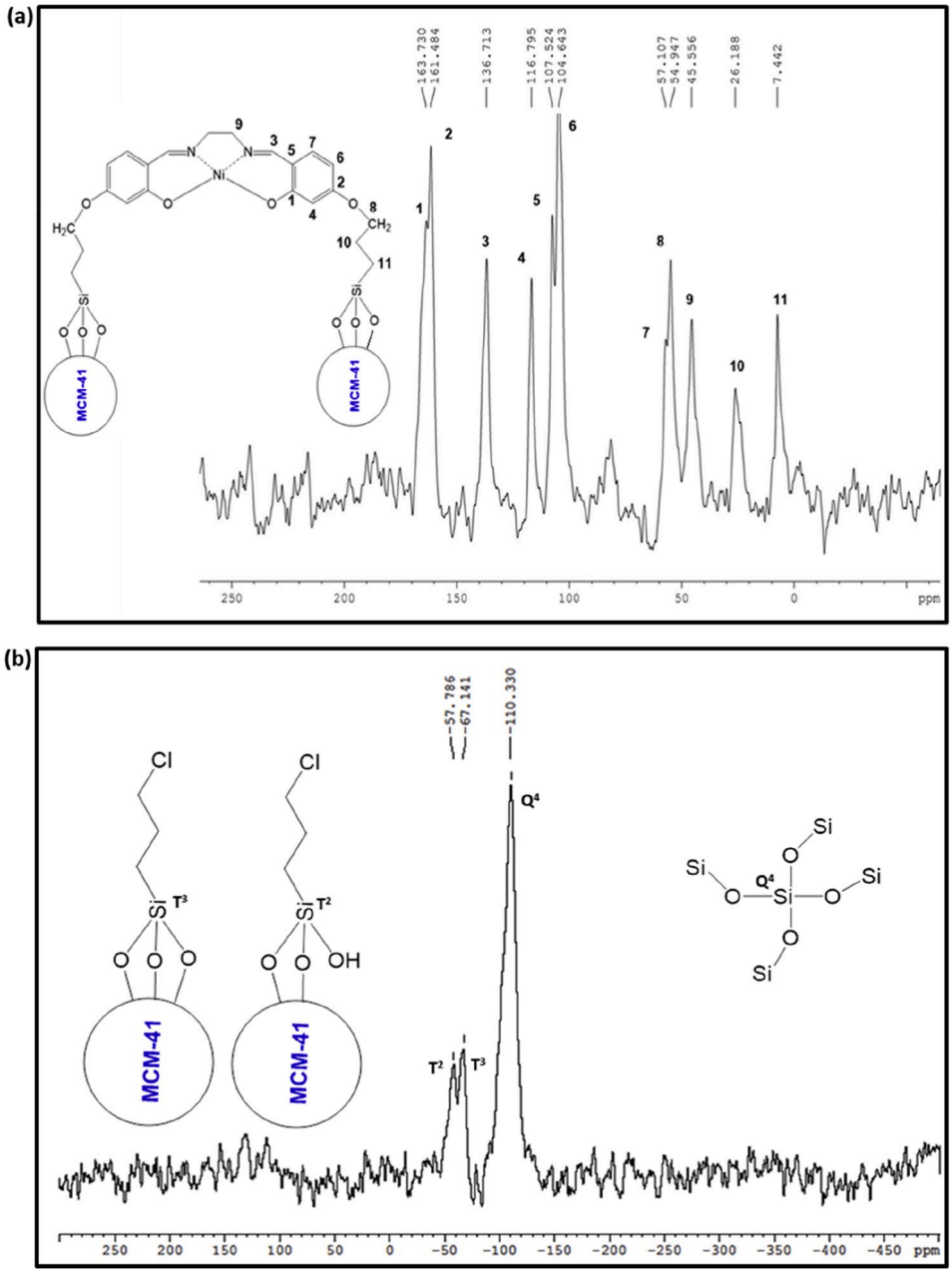

Fig. 2. The solid state MAS NMR spectra of (a) ^{13}C and (b) ^{29}Si for MCMSalenNi.

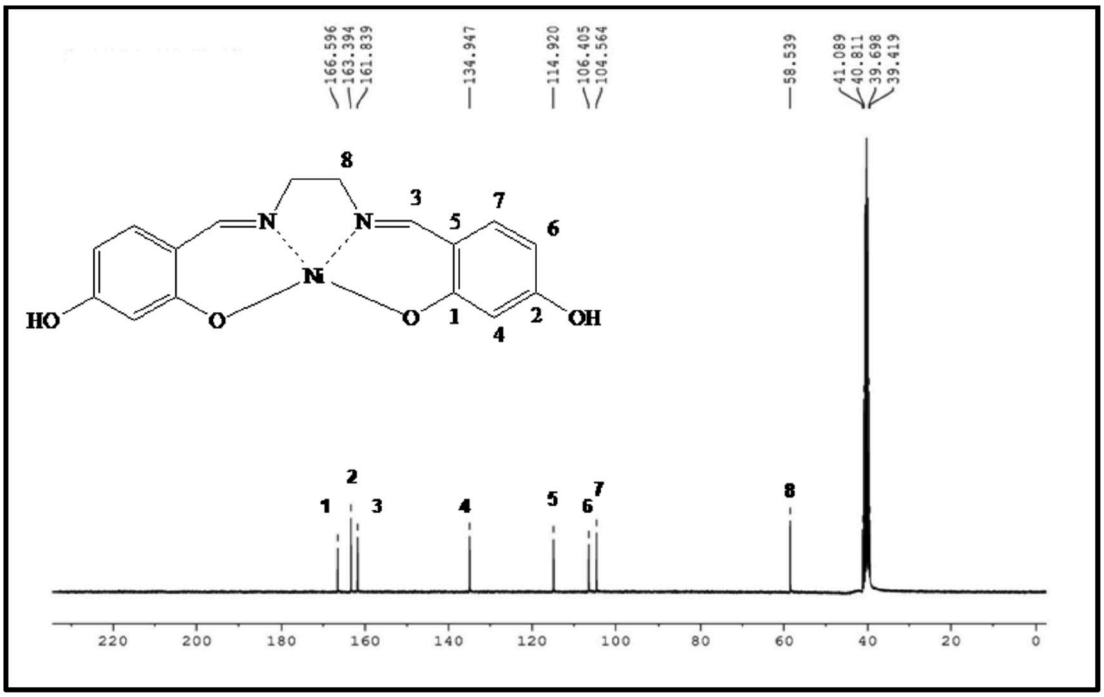

Fig. 3. The ^{13}C liquid state NMR of Ni(4-OH)$_2$ salen complex in DMSO-d_6 (125 MHz).

peaks corresponding to the (Si(OSi)$_2$OH$_2$) and (Si(OSi)$_3$OH) moieties were not detected [35].

3.1.3. XRD analysis

The low angle XRD spectra for MCM-41, Cl-MCM-41 and MCMSalenNi is shown in Fig. 4. The typical diffraction peaks for MCM-41 are present at ~2.17°, 3.80°, 4.35° and 5.64° that correspond to the (100), (110), (200) and (210) planes respectively [35]. The intensity of the peaks for both Cl-MCM-41 and MCMSalenNi however, was low in comparison to MCM-41. The peak corresponding to the (210) plane was not observed for either of these samples. The presence of the peak at ~2.17° (100) due to with the presence of hexagonal mesoporous structure typical of MCM-41. This can be seen from the TEM images in Fig. 6 [10]. The intensity of this peak decreased after the functionalization with CPTES and Ni(4-OH)$_2$ salen complex, which could be due to filling up of the mesoporous honey-comb structure of MCM-41.

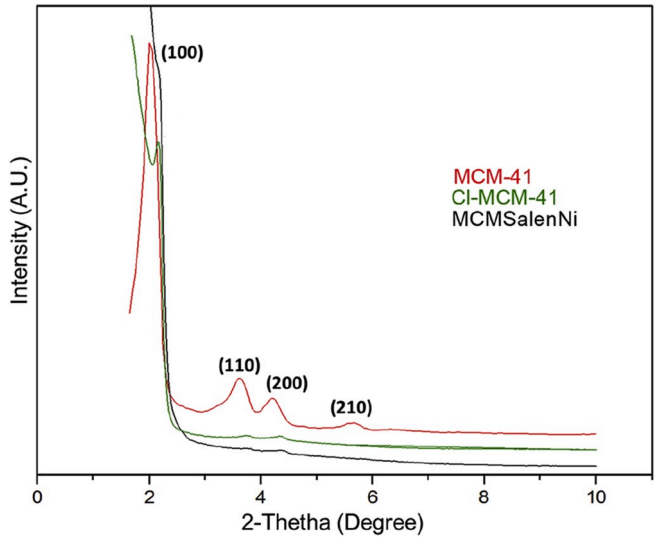

Fig. 4. The low angle XRD spectra of the samples prepared in the present study.

3.1.4. N_2 adsorption-desorption analysis

The N_2 adsorption-desorption plots of the samples are shown in Fig. 5 and their textural properties are shown in Table 3. All samples (MCM-41, Cl-MCM-41 and MCMSalenNi) exhibited type IV isotherm with H4 hysteresis loop, which is typical for mesoporous solids [32]. However, the volume of N_2 adsorbed ($cm^3\ g^{-1}$ STP) for both Cl-MCM-41 and MCMSalenNi exhibited a significant drop relative to MCM-41 as the relative pressure (P/P_o) was increased. This is consistent with the blocking of the hexagonal pores due to the large ligand molecules that has been attached onto the surface.

The surface area for MCM-41 was calculated to be 848 m^2g^{-1}. However, there was a sharp decrease in the surface area for Cl-MCM-41 and MCMSalenNi with 589 m^2g^{-1} and 503 m^2g^{-1} respectively. Nevertheless, the surface area of Cl-MCM-41 and MCMSalenNi was not much different. This should be consistent with the attachment of the Ni(4-OH)$_2$ complex onto the Cl-MCM-41 as shown in Scheme 1 earlier. Similar trends were also observed for the pore volume and pore width. These could be attributed to the blockage of the pores after functionalization, consequently reducing the specific surface area of the samples [10]. Despite the changes in the porosity of the samples post-functionalization, a narrow pore width distribution was still observed for both Cl-MCM-41 and MCMSalenNi which is typical for MCM materials [10].

3.1.5. TEM/SEM microscopy

The TEM images of the silica samples are shown in Fig. 6. It can be seen that the honey-comb structure of the MCM-41 (Fig. 6a) had been clearly preserved after functionalization with CPTES (Fig. 6b) and later with Ni(4-OH)$_2$ salen complex (Fig. 6c). In addition, all samples exhibited ordered porous structure consistent with previous work on MCM-41 [35]. The average wall thickness and pore width has also been calculated from the TEM images and displayed in Table 3. The average

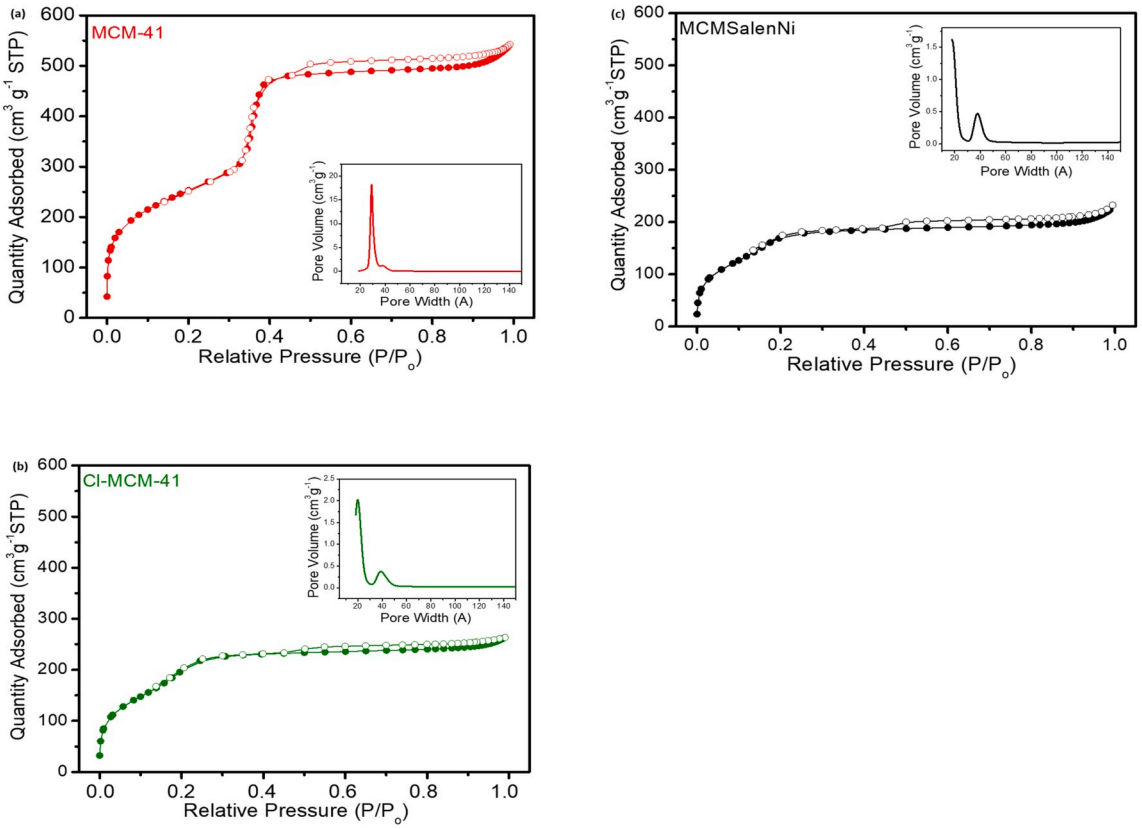

Fig. 5. The N_2 adsorption-desoprtion isotherm plots of (a) MCM-41, (b) Cl-MCM-41 and (c) MCMSalenNi with the pore size distribution (inset).

Table 3
Textural properties of the samples prepared in the present study.

Sample	N_2 adsorption-desoprtion analysis			XRD		TEM	
	Surface Area (m^2g^{-1})	Pore Volume (cm^3g^{-1})	Pore Width (nm)	d_{100} (nm)	Pore-Pore distance (a_o, nm)	Wall thickness (nm)	Pore Width (nm)
MCM-41	848	0.84	3.2	4.39	5.07	1.66	2.28
Cl-MCM-41	589	0.33	2.4	4.07	4.70	2.23	2.02
MCMSalenNi	503	0.26	2.2	4.06	4.69	2.39	1.76

pore width however, seemed to have differed slightly from that of the N_2 adsorption-desoprtion analysis. This could probably be due to the N_2 adsorption-desorption analysis being more quantitative and thorough compared to that of TEM hence probably more accurate.

The SEM images of MCM-41 and Cl-MCM-41 are depicted in Fig. 7 (a & b) and appeared to be smooth with cylindrical particles forming agglomeration. This is typical for mesoporous silica though for MCMSalenNi (Fig. 7c), jagged surface was observed. This could be due to the functionalization with the $Ni(4\text{-}OH)_2$salen complex. In addition, EDX analysis was performed and it was found that the nickel content from the functionalization of $Ni(4\text{-}OH)_2$ salen complex was ~8.2%. This value was in close agreement to the one obtained from AAS analysis (7.8%).

3.2. Oxidation of benzyl alcohol using MCMSalenNi

The oxidation of benzyl alcohol into benzaldehyde was studied using MCMSalenNi as a heterogeneous catalyst and the results are shown in Table 4. The conversion of benzyl alcohol increased from 85.6 to 98.4% as the temperature was hiked from 70 to 90 °C. Since periodic acid is a mild oxidant, slightly higher temperature was required for the optimal conversion of benzyl alcohol. The amount of catalyst was also varied from 0.0125 to 0.0625 g. The reaction conversion however, was at its highest when 0.05 g of MCMSalenNi was used. Further increase in the amount of catalyst only resulted in reduced conversion. This could be due to mass transfer limitations due to high dosage of the catalyst, as reported previously [36].

The ratio of benzyl alcohol to periodic acid was also varied (1:0.5 mmol, 1:0.25 mmol, entry 7 and 8 in Table 4). The result showed that when the ratio was 1:0.25, there was sharp a decrease in the conversion of benzyl alcohol. This shows that a ratio of 1:0.50 was the optimum to obtain the maximum conversion of benzyl alcohol. Apart from that, two other oxidants (hydrogen peroxide and tert-butyl hydroperoxide, entry 10 and 11 in Table 4) were also used. These resulted in very low conversion with no traces of benzaldehyde. This could probably be due to the high reactivity of these oxidants. These oxidants would probably dissociate extremely fast in the presence of MCMSalenNi at 70 °C that it was ineffective in oxidizing benzyl alcohol into benzaldehyde. Hence, a

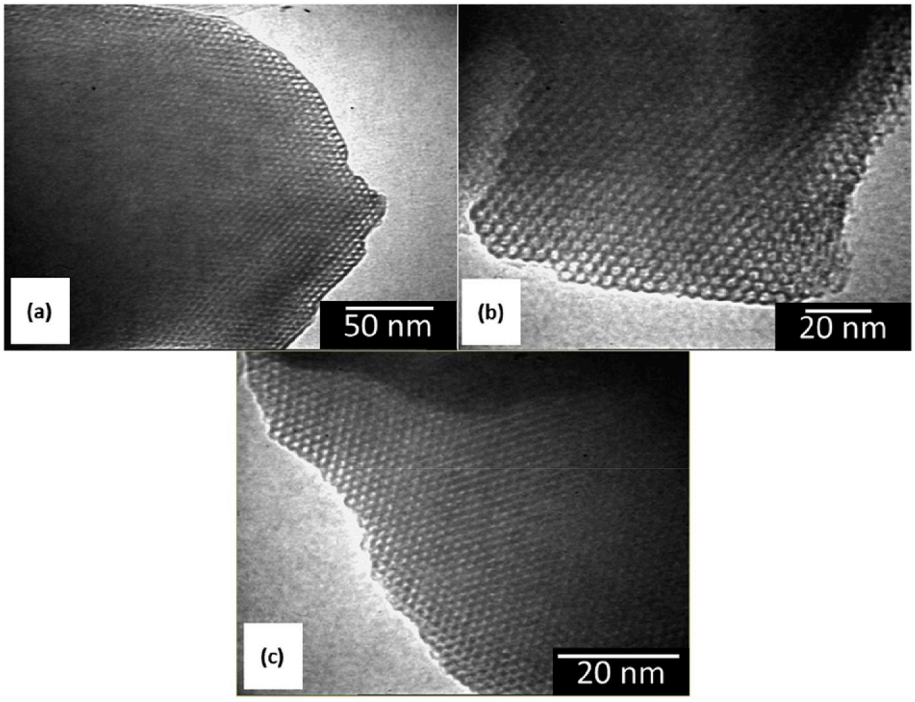

Fig. 6. The TEM images of (a) MCM-41, (b) Cl-MCM-41 and (c) MCMSalenNi.

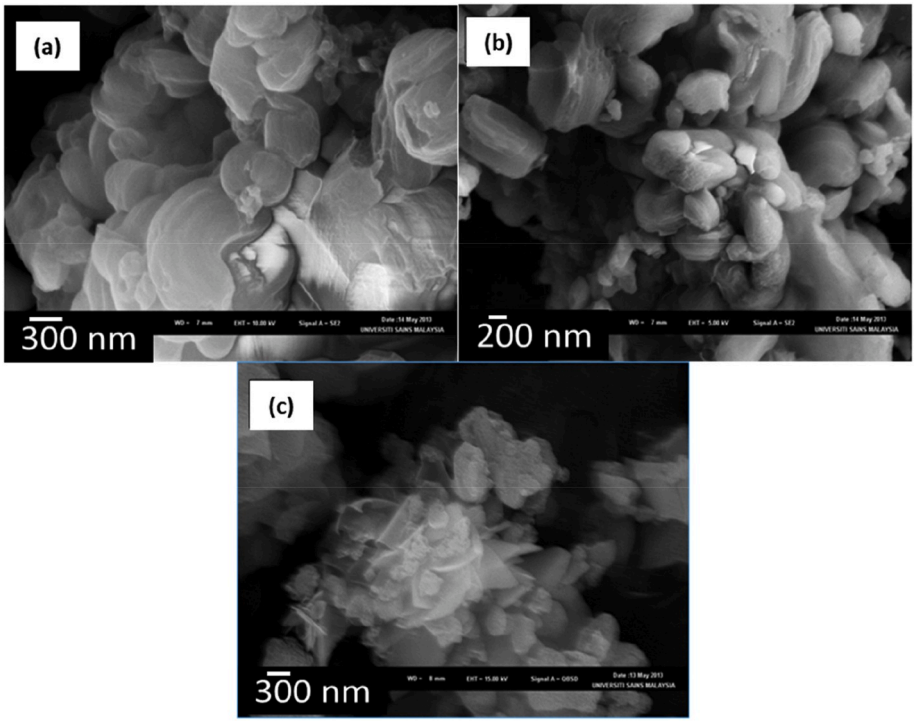

Fig. 7. The SEM images of (a) MCM-41, (b) Cl-MCM-41 and MCMSalenNi.

Table 4
The optimization of parameters for the oxidation of benzyl alcohol using MCMSalenNi as heterogeneous catalyst.

Entry	Catalyst amount (g)	Temp. (°C)	Time (min)	Conversion %	Selectivity %
1	0.05	70	90	85.6	59.0
2	0.05	80	90	91.4	53.3
3	0.05	90	90	98.4	48.8
4	0.0125	90	90	72.2	47.0
5	0.025	90	90	95.3	52.9
6	0.0625	90	90	96.2	49.7
7[b]	0.05	90	90	81.5	54.1
8[c]	0.05	90	90	35.9	70.0
9[d]	0.023	90	90	72.4	61.5
10[e]	0.05	70	240	4.8	–
11[f]	0.05	70	120	9.0	–

Reaction conditions: benzyl alcohol (1 mmol), periodic acid (1 mmol), acetonitrile (12 mL) with varying temperatures.
[b,c] Ratio of benzyl alcohol:periodic acid (1:0.5 mmol) and (1:0.25 mmol) respectively.
[d] Using Ni(4-OH)$_2$ salen complex as a homogenous catalyst under optimized conditions.
[e,f] Using H_2O_2 and t-BuOOH as oxidant respectively.

milder oxidant such as periodic acid is preferred [37]. The Ni(4-OH)$_2$ salen complex was used as a homogeneous catalyst for comparison. The conversion of benzyl alcohol was only ~72.4%. Therefore, the heterogenization of the salen complex was essential to produce a more efficient catalyst, i.e. MCMSalenNi.

3.3. Leaching and reusability studies on MCMSalenNi

The catalyst showed signs of leaching once it was removed from the reaction mixture after 15 min and the reaction was allowed to proceed. Fig. 8 shows that when the catalyst was removed, the conversion of benzyl alcohol was approximately 35% and it reached a plateau of 57.0% after 90 min of reaction time. Although there was an increase in the conversion of about 22% (after removal of the catalyst), the fact that it reached a plateau and never reached the maximum of 98%, shows that leaching was minimal.

The reusability studies of MCMSalenNi was carried out over several runs as shown in Fig. 9. The conversion of benzyl alcohol showed a decrease from 98.4 to 80.8% percent after six subsequent runs. The

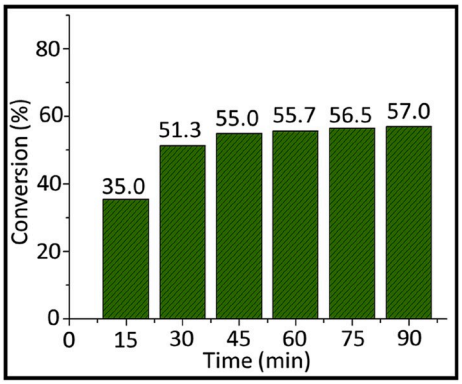

Fig. 8. The leaching test carried out using MCMSalenNi during the oxidation of benzyl alcohol.

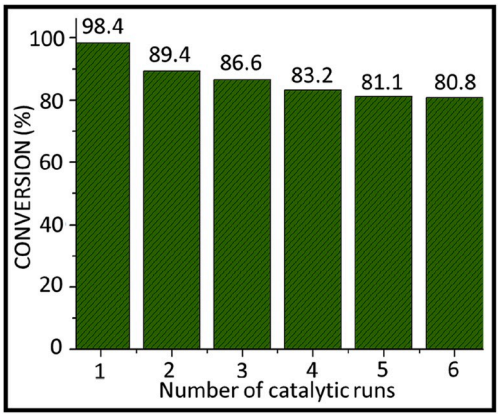

Fig. 9. The reusability studies conducted with MCMSalenNi under optimized conditions.

conversion of benzyl alcohol seemed to have reached a plateau upon successive reuse further proving that the leached material was not the functionalized Ni(4-OH)$_2$ salen complex but that which had been physically adsorbed on the surface of the mesoporous silica support. This also shows that the catalyst is stable upon successive reuse without much loss in its activity.

3.4. Proposed reaction mechanism

The proposed mechanism for the catalytic oxidation of benzyl alcohol is shown in Scheme 2. Orthoperiodic acid (H_5IO_6) might have underwent dissociation, forming metaperiodic acid (HIO_4).. The cationic Ni^{2+} species serves as the reactive center in attracting the electronegative oxygen atoms of the metaperiodic acid and benzyl alcohol forming a stable octahedral configuration (iii). The condensation reaction would take place between metaperiodic acid and benzyl alcohol on the surface of the catalyst resulting in the loss of water molecule. Simultaneously, the α-hydrogen from the deprotonated benzyl alcohol would be abstracted by the oxygen atom of the fragmented metaperiodic acid forming iodic acid via S_N2 reaction. The loss of the α-hydrogen from the deprotonated benzyl alcohol molecule would consequently result in the formation of benzaldehyde.

4. Conclusions

In conclusion, Ni(4-OH)$_2$ salen complex was successfully synthesized and functionalized onto MCM-41 derived from RH with the aid of CPTES as an alkylating agent. The ^{13}C and ^{29}Si MAS NMR proved that the functionalization had indeed taken place. The catalyst, MCMSalenNi, was tested in the oxidation of benzyl alcohol using periodic acid as a mild oxidant. A high conversion was obtained (~98%) within 90 min of reaction at 90 °C with 48.8% selectivity towards benzaldehyde. Furthermore, the catalyst was stable and able to be reused six times without significant loss of activity despite some leaching due to the physically adsorbed active material.

Declaration of competing interest

The authors openly express there is no conflict of interest in the submission of the current work.

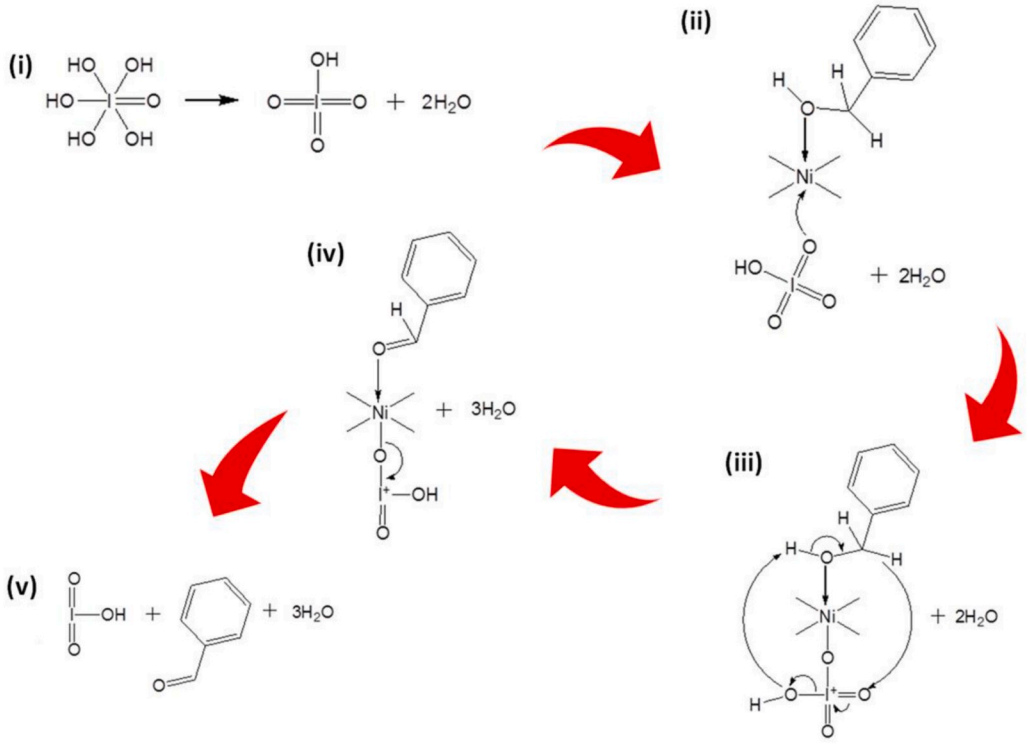

Scheme 2. The proposed mechanism for the oxidation of benzyl alcohol using MCMSalenNi as heterogeneous catalyst and periodic acid as oxidant.

CRediT authorship contribution statement

Salih Hamza Abbas: Methodology, Investigation, Writing - original draft. **Farook Adam:** Supervision, Project administration, Funding acquisition. **Lingeswarran Muniandy:** Visualization, Data curation, Writing - review & editing.

Acknowledgements

The authors would like to take this opportunity to thank the Government of Malaysia for the RU grant (Ac. No. 1001/PKIMIA/811269) which partly supported this work. S. H. Abbas would also like to thank the Basrah University, Republic of Iraq for the study leave.

References

[1] B.F. Santos, M.A. Correa, M. Chorili, Brazilian Journal of Pharmaceutical Sciences 51 (2015) 17–26.
[2] C. Juliano, G.A. Magrini, Cosmetics 5 (2018) 19–36.
[3] A. Dixit, P. Pandey, R. Mahajan, D.C. Dhasmana, Res. J. Pharmaceut. Biol. Chem. Sci. 5 (2014) 558–563.
[4] M.J. Lima, M.J. Sampaio, C.G. Silva, A.M.T. Silva, J.L. Faria, Catal. Today 328 (2019) 293–299.
[5] C. Lu, J. Hu, Y. Meng, A. Zhou, F. Zhang, Z. Zhang, Chem. Eng. Res. Des. 141 (2019) 181–186.
[6] M.J. Lima, A.M.T. Silva, C.G. Silva, J.L. Faria, J. Catal. 353 (2017) 44–53.
[7] G.D. Yadav, G.P. Fernandes, Catal. Today 207 (2013) 162–169.
[8] T.-H. Liou, Carbon 42 (2004) 785–794.
[9] A.A. Ahmed, F. Adam, Microporous Mesoporous Mater. 103 (2007) 284–295.
[10] L. Muniandy, F. Adam, N.R.A. Rahman, E.-P. Ng, Inorg. Chem. Commun. 104 (2019) 1–7.
[11] N.K. Renuka, A.K. Praveen, K. Anas, Mater. Lett. 109 (2013) 70–73.
[12] S. Mukherjee, S. Barman, G. Halder, Groundwater for Sustainable Development 7 (2018) 39–47.
[13] M.A. Jayan, S.S. Dawn, G.G.V. Kumar, Mater. Lett. 240 (2019) 55–58.
[14] Y. Sim, J. Yoo, J.-M. Ha, J.C. Jung, Journal of Energy Chemistry 35 (2019) 1–8.
[15] E. Nehlig, L. Motte, E. Guenin, RSC Adv. 5 (2015) 104688–104694.
[16] N.T. Thao, N.T. Nhu, J. Sci.: Advanced Materials and Devices 3 (2018) 289–295.
[17] S.S.P. Sultana, R. Ali, M. Kuniyil, M. Khan, A. Alwarthan, D.H.V. Kishore, M. E. Assal, K.R.S. Prasad, N. Ahmad, M.R.H. Siddiqui, S.F. Adil, Journal of Saudi Chemical Society 21 (2017) 878–886.
[18] M. Kimi, M.M. Hadi Jaidie, S.C. Pang, J. Phys. Chem. Solid. 112 (2018) 50–53.
[19] J. Liu, S. Zou, J. Wu, H. Kobayashi, H. Zhao, J. Fan, Chin. J. Catal. 39 (2018) 1081–1089.
[20] G. Wu, Y. Gao, F. Ma, B. Zheng, L. Liu, H. Sun, W. Wu, Chem. Eng. J. 271 (2015) 14–22.
[21] A.J. Faqeeh, T.T. Ali, S.N. Basahel, K. Narasimharao, Molecular Catalysis 456 (2018) 10–21.
[22] F. Adam, H. Osman, K.M. Hello, J. Colloid Interface Sci. 331 (2009) 143–147.
[23] T. Radhika, S. Sugunan, J. Mol. Catal. Chem. 250 (2006) 169–176.
[24] F. Adam, J.-H. Chua, J. Colloid Interface Sci. 280 (2004) 55–61.
[25] P. Sutra, D. Brunel, Chem. Commun. 1 (1996) 2485–2486.
[26] A. Arola-Arnal, J. Benet-Buchholz, S. Neidle, R. Vilar, Inorg. Chem. 47 (2008) 11910–11919.
[27] S. Bhattacharjee, T.J. Dines, J.A. Anderson, J. Catal. 225 (2004) 398–407.
[28] S. Bhattacharjee, J.A. Anderson, J. Mol. Catal. Chem. 249 (2006) 103–110.
[29] X.-H. Lu, Q.-H. Xia, H.-J. Zhan, H.-X. Yuan, C.-P. Ye, K.-X. Su, G. Xu, J. Mol. Catal. Chem. 250 (2006) 62–69.
[30] F. Adam, M.S. Batagarawa, Appl. Catal. Gen. 454 (2013) 164–171.
[31] F. Adam, J. Andas, I.A. Rahman, Chem. Eng. J. 165 (2010) 658–667.
[32] F. Adam, A. Iqbal, Chem. Eng. J. 160 (2010) 742–750.
[33] B.B. Fan, H.Y. Li, W.B. Fan, C. Jin, R.F. Li, Appl. Catal. Gen. 340 (2008) 67–75.
[34] N.V. Tverdova, N.I. Giricheva, G.V. Girichev, N.P. Kuz'mina, O.V. Kotova, A. V. Zakharov, Russ. J. Phys. Chem.: Structure of Matter and Quantum Chemistry 83 (2009) 2255–2265.
[35] J.N. Appaturi, F. Adam, Appl. Catal. B Environ. 136–137 (2013) 150–159.
[36] M.R. Maurya, S.J.J. Titinchi, S. Chand, J. Mol. Catal. Chem. 214 (2004) 257–264.
[37] L. Muniandy, F. Adam, M.A. Rahman, A. Iqbal, N.R.A. Rahman, Appl. Surf. Sci. 398 (2017) 43–55.